

FIG. 6. Excitation function for $\lambda 4603.7$. A, 5-min. exposure; B, 30-min. exposure. Relative intensity of 100 taken at 43 volts.

For the two lines, $\lambda\lambda 4264.7$ and 4763.6 whose classifications are not given in Table II a consideration of the forms of their optical excitation functions, of their onset potentials, and of their wave-lengths when considered in the light of the energy level scheme leads to the suggestion that they may be due to transitions of the types, $5p^5(^2P_{1/2})6d$, $7s-5p^5(^2P_{1/2})6p$ and $5p^5(^2P_{3/2})6d$, $7s-5p^5(^2P_{3/2})6p$, respectively.

In conclusion I wish to express my thanks to Dr. J. T. Tate who suggested the problem, to Dr. J. Valasek for helpful suggestions, to Dr.

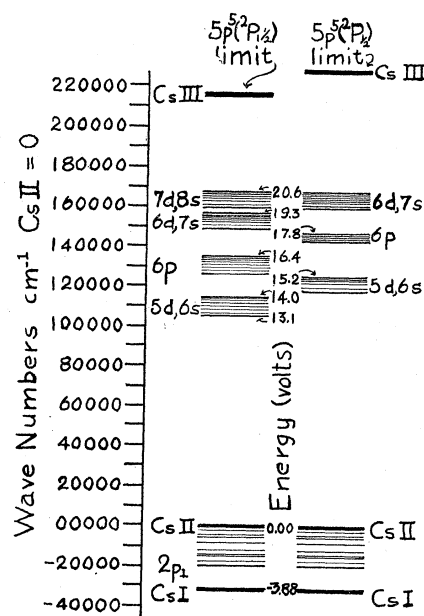


FIG. 7. Energy level scheme.

H. A. Erikson for the use of apparatus, and to the RCA Radiotron Corporation and the Bell Telephone Laboratories who furnished me with the necessary oxide-coated cathodes as well as some oxide-coated ribbon.

Isotopic Constitution of Lead from Hyperfine Structure

JOHN L. ROSE AND R. K. STRANATHAN, *Department of Physics New York University, University Heights*

(Received April 22, 1936)

The relative abundance of the isotopes of lead was determined from intensity measurements of the hyperfine structure components of the lead spark line $\lambda 5372$. With eleven calibrated wire screens a single order of the Fabry-Perot interference pattern was photographed with the same exposure time for each screen. The following results from densitometer measurements were obtained for the

percentage abundance of the isotopes of ordinary lead: 51.5, 26.3, 21.4 and 0.8 for Pb^{208} , Pb^{206} , Pb^{207} , and Pb^{204} , respectively. For integral masses of the isotopes the mean mass number is 207.22. Assuming a packing factor of +1, this number when converted to the chemical atomic weight scale becomes 207.20.

IT has been shown by several investigators¹⁻⁴ that spectral lines for the isotopes Pb^{204} , Pb^{206} and Pb^{208} , each with nuclear spin $I=0$, are always single but the lines for Pb^{207} , with

spin $I=\frac{1}{2}$, may have as many as four components depending on the J values and splittings of the initial and final atomic energy levels. It has been possible to make very rough esti-

¹ H. Kopfermann, *Zeits. f. Physik* **75**, 363 (1932).

² J. L. Rose and L. P. Granath, *Phys. Rev.* **40**, 760 (1932).

³ H. Schüler and E. G. Jones, *Zeits. f. Physik* **75**, 563 (1932).

⁴ J. L. Rose, *Phys. Rev.* **47**, 122 (1935).

mates of the relative abundance of the above isotopes for several samples of lead by visually observing the intensities of components of the Fabry-Perot interference patterns of various lines. The four isotopes observed in the hyperfine structure patterns have the same order of abundance and are the four more abundant of the eight isotopes reported by Aston⁵ for ordinary lead.

Many difficulties peculiar to lead were experienced by Aston in making an analysis of the isotopic constitution with the mass spectrograph. The presence of mercury and hydrogen in the tube was also very troublesome. The lighter and less abundant isotopes of lead could not be detected with certainty if a small amount of mercury were present in that the heavier isotopes of the latter have the same mass. Corrections had to be made for the blackening thought to be due to the heavier lead isotopes because the hydrogen from the decomposed lead tetramethyl in the source formed hydrides. After corrections were made the following figures were found by Aston to represent the percentage abundance of the isotopes of ordinary or common lead:

Mass numbers.....	203,	204,	205,	206,	207,	208,	209,	210
Abundance.....	0.04,	1.50,	0.03,	27.75,	20.20,	49.55,	0.85,	0.08

The mean mass number for these values is 207.190.

There is a question of the existence of Pb²⁰⁹ and Pb²¹⁰ in ordinary lead. The blackening of the plate thought to be due to these may have been produced entirely by hydrides. One would not expect to find nonradioactive Pb²¹⁰ in ordinary lead since a radioactive isotope (Ra D) of the same mass is known to exist. Later, Aston⁶ found no evidence of this isotope. However, his discharge tube was operating rather unsatisfactorily. A. J. Dempster⁷ with his new "achromatic" mass spectrograph has found no evidence of Pb²⁰⁹. As yet he has been able to observe only the four more abundant isotopes reported above. K. T. Bainbridge and E. B. Jordan⁸ working with a high dispersion linear scale mass spectro-

graph and a source free of hydrogen could have detected with certainty Pb²⁰⁹ if it had existed to the extent of 1/10 that reported by Aston. Two different methods of measurement used by them agreed in indicating that 1/30 of the reported 0.85 percent abundance could just have been detected. If this isotope exists in the same order of abundance as that of Pb²⁰⁴ its presence should be detected with certainty in the hyperfine structure pattern of $\lambda 4386$, shown in Fig. 1.

It appears that ordinary lead with the possible exception of about one part in a thousand is composed of the four isotopes which have been observed in hyperfine structure patterns. Photometric measurements of the relative intensities of the components of the Fabry-Perot patterns for certain lines should therefore give a very good result for the abundance of Pb²⁰⁴, Pb²⁰⁶, Pb²⁰⁷ and Pb²⁰⁸ if we neglect the other possible isotopes.

ISOTOPE DISPLACEMENTS AND Pb²⁰⁴

Schüler and Jones³ were the first to observe in the hyperfine structure patterns of $\lambda\lambda 7228$, 5609, 5201 and 5005 a faint component which indicated the presence of Pb²⁰⁴ in ordinary lead. One of us (J.L.R.) was not able to observe this component in a previous investigation⁴ because faint ghosts, peculiar to the etalon plates used at that time, appeared in the position of the expected 204 component for orders near the center. Another pair of plates was used in the present work for photographing two of the above lines and also $\lambda 4386$, whose pattern should show the 204 component. The faint component was found in the patterns of all three of these lines. The lines in which the 204 component can be observed directly have small isotope shifts, and as can be seen in Fig. 1 the faint 204 component is too close to more intense components for accurate densitometer measurements. All other lines favorable for intensity measurements have patterns in which the more intense 207 component is very near the position for 204. The relative intensity of the 207 components is known from the sum rule and if 204 and the stronger 207 are close enough together not to be resolved by the interferometer, this type of pattern can be used for a determination of the isotopic constitution of lead as described below.

⁵ F. W. Aston, Proc. Roy. Soc. **A140**, 535 (1933).

⁶ F. W. Aston, Proc. Roy. Soc. **A149**, 396 (1935).

⁷ A. J. Dempster, Phys. Rev. **49**, 416A (1936).

⁸ K. T. Bainbridge and E. B. Jordan, Phys. Rev. **49**, 416A (1936).

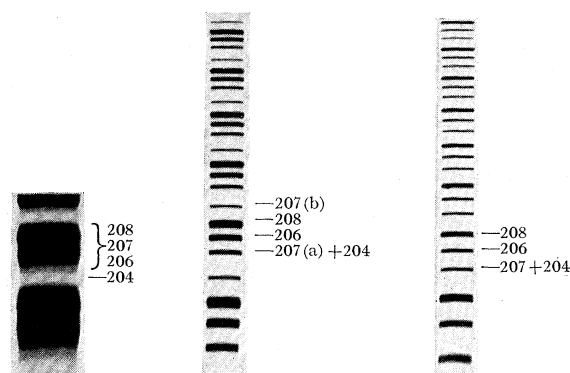


FIG. 1 (left). $\lambda 4386$, etalon spacer 17.193 mm.
 FIG. 2 (center). $\lambda 5372$, etalon spacer 3.561 mm.
 FIG. 3 (right). $\lambda 5372$, etalon spacer 5.194 mm.

It has been definitely shown from hyperfine structure measurements that the center of gravity of the 207 components is not at the midpoint between 206 and 208 as would be expected but for all patterns it is closer to 206 than to 208. The measured ratio of the separations of 206 and 208 from the 207 center of gravity is 0.63 ± 0.02 . The separations, 204 to 206 and 206 to 208, have been measured by Schüller and Jones³ in four lines. These separations and their ratios are shown in Table I.

TABLE I. Even isotope separations.

λ	204-206 $\Delta\nu$ cm^{-1}	206-208 $\Delta\nu$ cm^{-1}	204-206 206-208
5005	0.059	0.061	0.97
5201	0.065	0.072	0.90
5609	~ 0.046	0.052	~ 0.89
7228	0.084	0.088	0.96

It is interesting to note for these isotopes that the displacements are more what one would expect. The two measured separations are almost equal as shown by the ratio in the last column. The small isotope shifts and large differences of intensity of the components make the separations difficult to measure with accuracy and it may be that the actual ratio is unity. Also the blackening of the plate near 204 caused by the overexposure of 206 would make the center of gravity of the former appear to be closer to the latter than it actually is and thus tend to give a ratio from measured separations slightly less than unity. For the type of line discussed above in which the stronger 207(a) component is

very near to 204 the ratio of the separation 207(a)-206 to that of 206-208 is very nearly unity. The resolving power of the etalons used for these lines and the width of the components are such that 204 and 207(a) would be completely unresolved if the above ratio for the even isotopes were 1.00 ± 0.05 .

$\lambda 5372$ AND 5367 , Pb II

The spark line, $\lambda 5372$ ($p^2\ ^4P_{5/2} - 5F_{7/2}$), whose interference patterns for etalon spacers 3.561 and 5.194 mm are shown in Figs. 2 and 3, is perhaps the best line for intensity measurements. The $F_{7/2}$ level is single and all of the structure of $\lambda 5372$ is due to the $p^2\ ^4P_{5/2}$ level in which the separation of 206 and 208 is $0.283\ \text{cm}^{-1}$ and the splitting of 207 is $0.957\ \text{cm}^{-1}$. The line is very intense and sharp and shows no self-reversal in any of the stronger components even when the highest possible voltage is used to operate the hollow cathode source.⁴ It is ideal for visual observations and adjustments of the optical instruments and the spectral region is very favorable for silvered etalon plates.

With the exception of $\lambda 5367$ ($p^2\ ^4P_{5/2} - 5F_{5/2}$) which is ten to twenty times less intense than $\lambda 5372$, there are no lead or helium lines within 50A of $\lambda 5372$ so the slit of the Hilger constant deviation spectrograph may be opened wide without other lines overlapping. Fortunately $\lambda 5372$ and 5367 have identical patterns. The $F_{5/2}$ level is single and therefore the structure of both lines is due to the same energy level. By carefully grinding and trying several invar etalon spacers it was found that the interference patterns of the two lines coincided exactly when spacers 3.561, 4.208 and 5.185 mm were used. This means that for a change of phase of unity between corresponding components in the two lines the change of spacer thickness must be 0.324 mm and therefore the separation of corresponding components is $15.4\ \text{cm}^{-1}$. The lateral separation of the patterns of the two lines due to the dispersion of the spectrograph is less than one-tenth the width of the image of the collimator slit which was used. This makes it possible to use a large microphotometer slit in recording the blackening in the center of the pattern where the spectrograph slit images of the two lines are completely overlapped.

MEASUREMENTS AND RESULTS

Eleven calibrated wire screens were used in obtaining the intensity calibrations. Each screen was placed near the source and care was taken that the source lens did not throw a shadow of the screen on the collimator slit. A cross slit was used on the plateholder and so adjusted that only one or two orders were allowed to fall on the Eastman 4G photographic plate. Most of the photographs were obtained using one order only, either the third or the fourth from the center. However, two orders were photographed on some plates to provide check measurements. Successive photographs were taken without the screens and then with each of the eleven screens, thus covering a range of from 100 to 14.8 percent transmission. The plateholder could be moved either vertically or horizontally, permitting the intensity marks to be placed near each other in a vertical line. The same exposure time was used for all photographs of a group, thus eliminating any consideration of the Schwarzschild factor. Although no absorption is to be expected for this line under such conditions, the intensity of the source was varied so that exposure times ranged from 1 to 4 minutes to provide a check. A full Fabry-Perot pattern was also obtained to ascertain the change in intensity from order to order

and thereby provide the necessary correction factor if the intensity did not prove to be the same for each order in the region used for the intensity marks. Densitometer traces of the intensity marks and the full pattern were obtained. See Fig. 4. Calibration curves, similar to the ones shown in Fig. 5 were plotted for all apparent components of the pattern. By comparing the transmissions, which are proportional to the true intensities, corresponding to any given galvanometer deflection, the ratios of the intensities of the apparent components were calculated. These ratios were obtained for various galvanometer deflections, using the portions of the curves which were approximately linear.

The ordinary lead pattern of $\lambda 5372$ consists of the four apparent components, 208, 206, 207(a) + 204, and 207(b). In addition, by the proper choice of spacers the 207(b) component of one order was made to fall on the 207(a) + 204 of the adjacent order. These patterns then consisted of three apparent components 208, 206, and 207 + 204. The various intensity ratios are shown in Table II.

In this table it is shown that the ratio of 207(b) to 207(a) + 204 is 0.671. From the sum rule for intensities, the ratio of 207(b) to 207(a) for $\lambda 5372$ and 5367 is known to be 5 to 7 or 0.714. The difference in these ratios is due to the

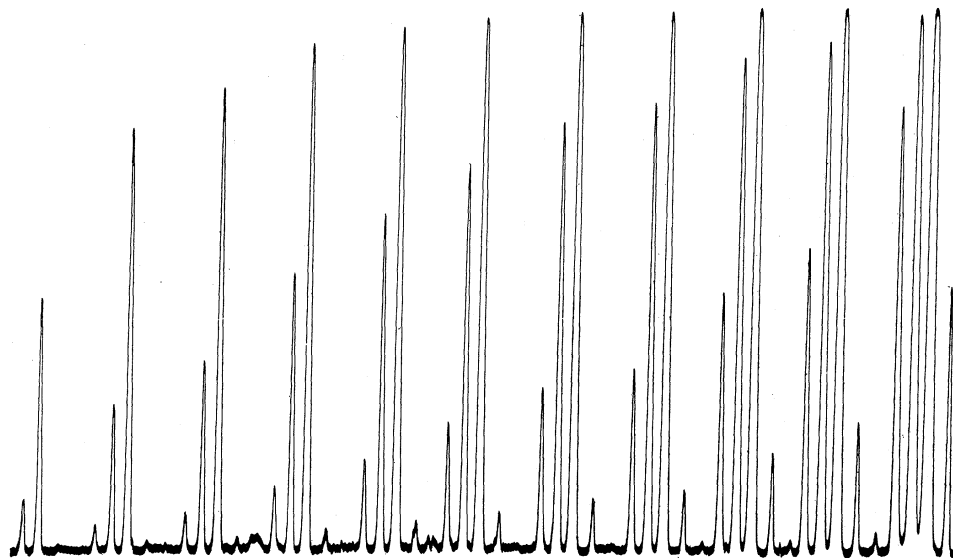
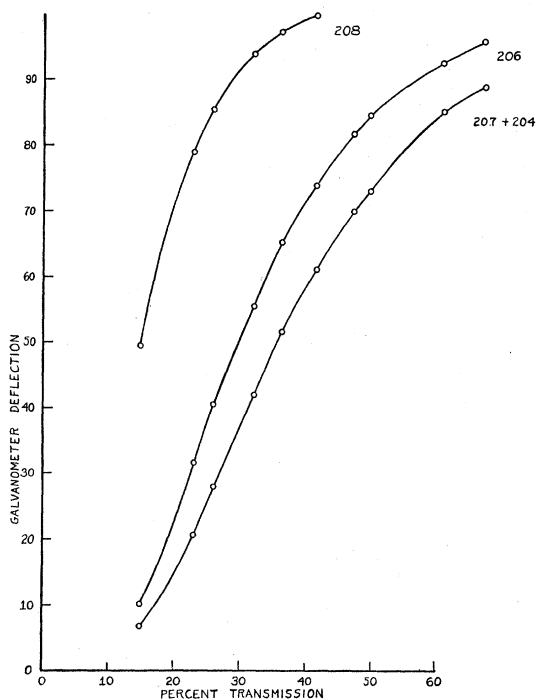


FIG. 4. Microphotometer trace of a single order of $\lambda 5372$ for plate No. 22. Percentage transmissions: 100.0, 67.3, 61.0, 49.8, 47.3, 41.6, 36.3, 32.1, 25.9, 22.9, 14.8.

TABLE II. Measured intensity ratios in percent.

PLATE	SPACER (mm)	$\frac{206}{208}$	NO. OF VALUES	$\frac{207(a)+204}{206}$	NO. OF VALUES	$\frac{207(b)}{207(a)+204}$	NO. OF VALUES	$\frac{207+204}{206}$	NO. OF VALUES
37	3.561	50.6	8	50.8	15	67.2	19		
35	3.561	50.9	8	50.0	11	66.9	13		
22	3.561	50.9	7	50.7	8				
42	5.194	51.5	11					84.1	19
32	5.194	51.2	15					84.0	21
40	4.172					67.3	21		
Average values		51.1 ₄		50.5 ₀		67.1 ₃		84.0 ₅	

FIG. 5. Intensity-blackening curves for plate No. 42. Single order of $\lambda 5372$, etalon spacer 5.194.

204 component which coincides with 207(a) in the hyperfine structure of these lines and therefore it is possible to determine the relative abundance of Pb^{207} to Pb^{204} . This was found to be 26.6 : 1.0. With this ratio and the densitometer data in columns 3 and 9 of Table II the percentage abundance for all the observable isotopes can be calculated. The results are shown below :

Mass Number.....	208	207	206	204
Abundance.....	51.5	21.3	26.3	0.8

The mean mass number from these figures assuming the masses of the isotopes to be integral is 207.22₈. The same mean mass number was found by using the data in column 5 instead of those in column 9 which were used above.

The packing fraction for lead is not accurately known but Aston⁵ has estimated the probable value to be between 0 and +1. The conversion factor from the chemical to the physical scale seems to be as large as 1.00025. When the above calculated mean mass number is corrected for a packing factor of +1 and then converted to the chemical scale the value becomes 207.20. This is lower than the present international chemical atomic weight 207.22. Unless this chemical atomic weight is too high the necessary packing fraction correction for agreement of the atomic weights obtained by the two methods is considerably greater than the value estimated by Aston. If Pb^{204} is more abundant than 0.8 percent the difference between the two would be still larger. It appears that this result for Pb^{204} which has to be at least the minimum abundance in order to account for the ratios in column 7 of Table II is very nearly correct.

In conclusion the authors wish to express their appreciations and thanks to Dr. R. L. Garman of the Department of Chemistry, Washington Square College, for his interest and extreme care in microphotometering the photographed etalon patterns and to the National Research Council for a grant-in-aid for hyperfine structure investigations.

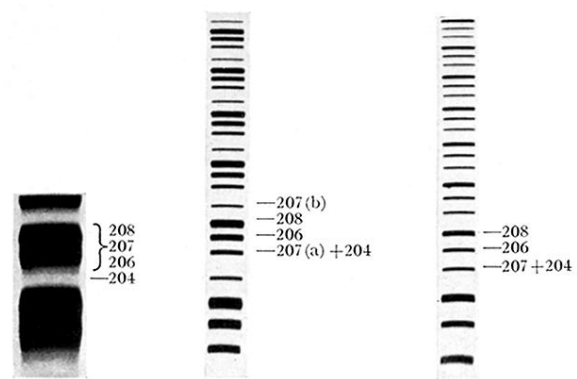


FIG. 1 (*left*). $\lambda 4386$, etalon spacer 17.193 mm.
 FIG. 2 (*center*). $\lambda 5372$, etalon spacer 3.561 mm.
 FIG. 3 (*right*). $\lambda 5372$, etalon spacer 5.194 mm.